

# Size matters, but not for everyone: Individual differences for contrast discrimination

Tim S. Meese

Vision Sciences, Aston University,  
Birmingham, United Kingdom



Robert F. Hess

McGill Vision Research, Department of Ophthalmology,  
McGill University, Montreal, Quebec, Canada



Cristyn B. Williams

McGill Vision Research, Department of Ophthalmology,  
McGill University, Montreal, Quebec, Canada

It is very well known that contrast detection thresholds improve with the size of a grating-type stimulus, but it is thought that the benefit of size is abolished for contrast discriminations well above threshold [e.g., Legge, G. E., & Foley, J. M. (1980)]. Here we challenge the generality of this view. We performed contrast detection and contrast discrimination for circular patches of sine wave grating as a function of stimulus size. We confirm that sensitivity improves with approximately the fourth-root of stimulus area at detection threshold (a log–log slope of  $-0.25$ ) but find individual differences (IDs) for the suprathreshold discrimination task. For several observers, performance was largely unaffected by area, but for others performance first improved (by as much as a log–log slope of  $-0.5$ ) and then reached a plateau. We replicated these different results several times on the same observers. All of these results were described in the context of a recent gain control model of area summation [Meese, T. S. (2004)], extended to accommodate the multiple stimulus sizes used here. In this model, (i) excitation increased with the fourth-root of stimulus area for all observers, and (ii) IDs in the discrimination data were described by IDs in the relation between suppression and area. This means that empirical summation in the contrast discrimination task can be attributed to growth in suppression with stimulus size that does not keep pace with the growth in excitation.

Keywords: human vision, inhibition, lateral interactions, masking, suppression, surround

## Introduction

Psychophysical contrast sensitivity is typically measured using a two-interval forced-choice paradigm in which observers discriminate between a null stimulus interval and an interval containing a test grating with contrast  $\Delta C$ . The reciprocal of  $\Delta C$  that corresponds with some criterion level of performance (e.g., 75% correct) is referred to as sensitivity. It is well known that sensitivity improves as the area of the stimulus is increased (Cannon, 1995; Graham, 1989; Howell & Hess, 1978; Luntinen, Rovamo, & Näsänen, 1995; Manahilov, Simpson, & McCulloch, 2001; Meese & Williams, 2000; Robson & Graham, 1981; Rovamo, Luntinen, & Näsänen, 1993, 1994; Polat & Tyler, 1999). This phenomenon is often attributed to probability summation between independent detectors; the greater the number of stimulated detectors, the greater is the probability of detecting the stimulus (Meese & Williams, 2000; Pelli, 1987; Robson & Graham, 1981; Tyler & Chen, 2000). But other explanations have also been offered, including physiological summation (Laming, 1988; Polat & Norcia, 1998; Polat & Tyler, 1999), matched filtering (Luntinen et al., 1995; Rovamo et al., 1993, 1994), facilitatory interactions (Bonneh

& Sagi, 1998; Polat & Norcia, 1998; Polat & Tyler, 1999), and nonlinear transduction followed by signal detection (Wilson, 1980), all of which remain possibilities.

Consider now how the experiment above can be extended to contrast discrimination. As before, the observer's task is to detect the presence of  $\Delta C$ , but this time in the presence of a pedestal grating (sometimes called a mask) with contrast  $C$ . In this situation, it has been found that so long as  $C$  is greater than a few percent, the detectability of  $\Delta C$  is largely independent of stimulus size (Legge & Foley, 1980). This is shown in Figure 1, where the relevant data from Legge and Foley have been replotted.

In some vision models, this change in relation between sensitivity and area with pedestal contrast has been achieved by disabling the summation process above threshold (Legge & Foley, 1980; Näsänen, Tiippana, & Rovamo, 1998; Swanson, Wilson, & Giese, 1984). But later models have been devised in which the transition arises much more smoothly (Cannon, 1995; Cannon & Fullenkamp, 1991a; Näsänen et al., 1998; McIlhagga & Pääkkönen, 1999; Meese, 2004). In most of these models, the abolition of area summation does not involve switching out or changing a process, but is an emergent property of the model's architecture. One example is the model developed by Meese (2004), which was based around a gain control equation

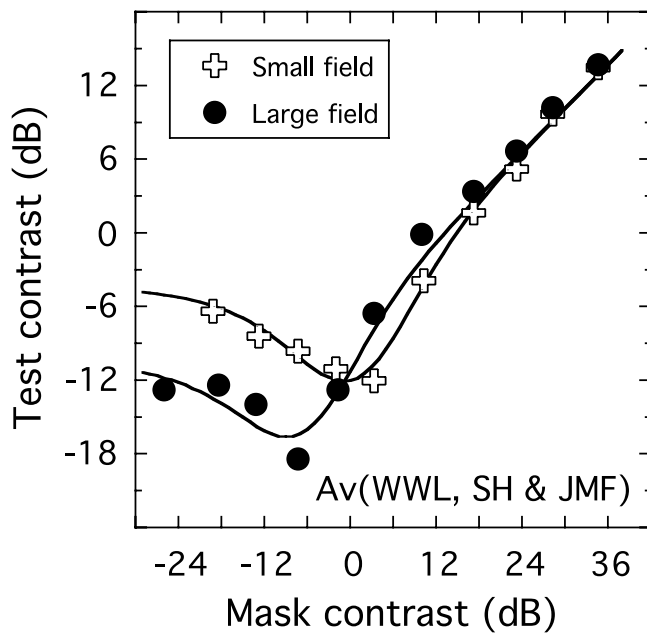


Figure 1. Contrast discrimination functions (average of three observers) for small (0.75 degrees wide) and large (6 degrees wide) field sizes, replotted from Legge and Foley (1980). Spatial frequency was 2 c/deg and stimulus duration was 200 ms. Here and elsewhere, contrast is expressed in decibels given by  $20 \log_{10}(C)$  re 1%, where  $C = 100(L_{\max} - L_{\min}) / (L_{\max} + L_{\min})$ . The small field condition was fit using the model described in the ‘area summation model’ subsection (Equations 2 and 3). There are four free parameters in this model, although following Legge and Foley the exponents  $p$  and  $q$  were preset to 2.4 and 2, respectively. The other two (sensitivity) parameters were estimated by a simplex algorithm that minimized the RMS error of the fit, giving  $\alpha_1 = 4.07$  and  $\beta_1 = 0.64$ . The model was then fit to the large field data using a single extra parameter that scaled the weights  $\alpha$  and  $\beta$  by a factor of 5.7 to give  $\alpha_2 = 23.2$  and  $\beta_2 = 3.65$ . This single size-scaling parameter captures three distinct features of the data: (i) area summation at low mask contrasts, (ii) the abolition of area summation at high mask contrasts, and (iii) the cross over of the dipper functions at intermediate mask contrasts. Formally equivalent models have been used to describe the similar data transformations seen in contrast adaptation (Meese, 2004; Meese & Holmes, 2002) and twin mask paradigms (Foley, 1994; Holmes & Meese, 2004).

introduced by Foley (1994). For the situation where the mask and test stimuli always have the same spatial and temporal characteristics, the observer’s sensory response to the stimulus can be expressed as follows:

$$\text{resp} = \frac{\sum_j (\eta_j c_j^p)}{Z + \sum_j (\mu_j c_j^q)} \quad (1)$$

The numerator and denominator contain strings of weighted ( $\eta_j$  and  $\mu_j$ ) contrast terms. These are often referred to as excitatory and suppressive terms and this is the terminology used here, although it should be borne in mind that other interpretations are possible (see [General discussion](#)). The excitatory and suppressive terms are raised to expansive powers  $p$  and  $q$ , respectively (typically,  $p - q \approx 0.4$ ) and summed across field position (indexed by  $j$ ). The denominator also contains a saturation constant ( $Z$ ), which is often set to 1 when the model’s degrees of freedom are expressed elsewhere in the model, as they are here.

At contrast detection threshold for a patch of grating, the denominator of Equation 1 is dominated by the saturation constant because other suppressive terms are negligible due to the low stimulus contrast. In this case, increasing the size of the grating patch increases only the level of excitation and area summation occurs. However, when the test increment is detected on a pedestal that is sufficiently suprathreshold, then the numerator and the denominator are dominated by the excitatory and suppressive contrast terms, respectively. For appropriate weightings of these terms, area summation can be abolished by a pedestal of moderate contrast and above because of its concomitant impact on excitatory integration and suppression. According to this model then, the weights of the contrast terms were in fact appropriately balanced (specifically,  $\sum_j \eta_j / \sum_j \mu_j$  was constant over  $j$ ) for the average observer in Legge and Foley’s (1980) contrast discrimination study, such that area summation appeared absent well above threshold. The success of this model is shown by the fit to Legge and Foley’s data replotted in Figure 1 (see figure caption for details).

But other experiments bring the generality of the precise balance of these weights into question. For example, several results from psychophysics (Cannon & Fullenkamp, 1991b, 1993; Ejima & Takahashi, 1985; Foley, 1994; Meese, 2004; Meese, Hess, & Williams, 2001; Olzak & Laurinen, 1999; Petrov, Carandini, & McKee, 2005; Snowden & Hammett, 1998; Xing & Heeger, 2000; Yu, Klein, & Levi, 2001) and fMRI (Williams, Singh, & Smith, 2003; Zenger-Landolt & Heeger, 2003) point to suppressive lateral interactions between mechanisms responding to co-oriented stimuli, such as a large patch of grating. One particularly relevant study here was that of Cannon and Fullenkamp (1993). They performed contrast matching of a central region of a stimulus in the presence of a co-oriented surrounding stimulus, for various contrasts of both center and surround. For some observers they found that certain surround configurations suppressed the perceived contrast of the center stimulus, whereas for other observers the same surround enhanced perceived contrast of the center. The authors interpreted their results in terms of competition between a suppressive process and facilitatory process and supposed that the balance between these two processes varied across observers. Of particular concern here is that

even for conditions in which the center and surround had the same contrast (meaning the contrast of a small patch of grating was being matched to a larger one), the level of contrast attenuation of the larger stimulus patch was not the same across observers.

These individual differences (IDs; see also [Results and discussion](#)) highlight an interesting possibility. If the introduction of a contrast pedestal abolishes empirical area summation (Legge & Foley, 1980) because of the precise balance of weights in a contrast gain control equation (Equation 1), then perhaps there are some observers whose weights are not balanced this way, and for whom area summation is not abolished.

We examined this by performing contrast detection and contrast discrimination experiments for four different sizes of circular patch of sine wave grating for several observers.

## Methods

### Equipment

Stimuli were stored in the framestore of a VSG2/3 or VSG2/4, and presentation was controlled by a Pentium PC. Stimuli were displayed on either (i) a NEC MultiSync XP17 monitor with mean luminance of 69 cd/m<sup>2</sup> and frame rate of 100 Hz; (ii) an Eizo F553-M monitor with mean luminance of 66 cd/m<sup>2</sup> and a frame rate of 120 Hz; or (iii) a Sony 20seII monitor with mean luminance of 62 cd/m<sup>2</sup> and a frame rate of 120 Hz. Look-up tables were used to perform gamma correction of the display monitors and the framestore was operated in either pseudo 12-bit mode (for the VSG2/3) or pseudo 15-bit mode (for the VSG2/4). Contrast is reported in percent given by  $C = 100[(L_{\max} - L_{\min}) / (L_{\max} + L_{\min})]$  and in decibels, given by  $20 \log_{10}(C)$  re 1%.

### Stimuli

In most experiments, stimuli consisted of a single circular patch of a vertical 1 c/deg sine wave grating. This was in sine phase with a small dark fixation point (4 pixels) in the center of the display that was visible throughout the experiment. The grating stimulus had its edges smoothed by a half period of a raised sine function. The sigmoidal ramp of the window was 1.25 degrees wide and the width of the window's half-amplitude was varied from 2.5 to 11.25 degrees, which we treat as the nominal stimulus diameter.

In the contrast discrimination experiments, the test stimulus was superimposed on a spatially identical pedestal stimulus with a contrast of 20% (26 dB). In the detection experiments, the pedestal stimulus had a contrast of 0%.

In [Experiment 3](#), several stimulus configurations were constructed from three basic stimulus patterns as follows. A small stimulus patch (S) was identical to the smallest

patch used in the earlier experiments (nominal diameter of 2.5 degrees). A large stimulus patch (L) was identical to the second largest stimulus patch in the main experiments (nominal stimulus diameter of 7.5 degrees). A doughnut-shaped stimulus (D) was created by subtracting the small stimulus (S) from the large stimulus (L). These three patterns were combined in different pairs of test and mask (with a contrast of 20%) to produce five stimulus configurations. A small stimulus was detected on a small pedestal (SS), a small stimulus was detected on a large pedestal (SL), a large stimulus was detected on a large pedestal (LL), a doughnut was detected on a doughnut pedestal (DD), and a doughnut was detected on a large pedestal (DL). In this experiment, the phase of the entire stimulus was shifted through 180 degrees on every trial to reduce the possibility of a build up of retinal afterimages.

In all experiments, stimulus duration was 100 ms and the viewing distance was 114 cm.

### Procedure

A temporal two-interval forced-choice (2IFC) technique was used and observers detected  $\Delta C$  in the presence of  $C$ , where  $C$  was 0% (contrast detection) or 20% (contrast discrimination). The computer determined the temporal interval that contained  $\Delta C$  randomly, and observers indicated their choice by pressing one of two buttons. The duration between the offset of the first interval and the onset of the second interval was 600 ms. A 'three-down, one-up' randomly interleaved staircase procedure (Cornsweet, 1962; Wetherill & Levitt, 1965; Meese, 1995) was used to control the magnitude of  $\Delta C$ . Estimates of threshold were made using probit analysis (Finney, 1971) to calculate the 75% correct point of psychometric functions based on about 100 trials accumulated over the last 12 'reversals' for each of a pair of interleaved staircases tracking the same condition. The data from the first pair of staircase reversals were always discarded. In different experiments, trials for different size conditions were either blocked or randomly interleaved (see next subsection). This gave a total of four different types of main experiment: blocked and interleaved designs for both contrast detection and contrast discrimination. Each observer took part in between 4 and 11 replications of the four size conditions in each type of experiment they performed. The data in the figures are the means and standard errors of these replications. When observers performed more than one type of experiment, each experiment was completed before a subsequent experiment was begun. Observers were also given at least 400 trials of practice before data collection began.

In all experiments, auditory feedback was used to indicate the correctness of response and the two temporal intervals were marked by short tones at the onset of the stimulus.

Data collection took place over an 8-year period between 1997 and 2005.

## Observers and order of experiments

The three authors (TSM, RFH, and CBW) served as observers for the detection experiment and the discrimination experiment in 1997. Two naïve observers also took part in both of these experiments (PAA and DHB). Both were postgraduate psychophysics students and were paid for the latter part of their contributions. All three authors performed the interleaved detection experiment before the interleaved discrimination experiment. PAA and DHB performed both types of discrimination experiment (interleaved, then blocked) before performing both types of detection experiment (interleaved, then blocked). PAA performed the interleaved discrimination experiment twice (in 2001 and 2004). In 2004, TSM performed all four types of experiment in the same order as DHB, repeating two of the experiments first performed in 1997. A further six naïve observers also performed the interleaved contrast discrimination experiment. Of these, DJH was a research assistant, RJS was a research fellow, PH and OH were postgraduate optometry students, JLD was an undergraduate optometry student who performed the experiment as part of her course requirement, and HYW was a paid volunteer. TSM, RFH, and DHB performed Experiment 3 in 2005. At this time, DHB was no longer naïve to the purpose of the conditions from the main experiment but was unaware of the purpose of the novel conditions in Experiment 3. All observers had normal or optically corrected to normal vision.

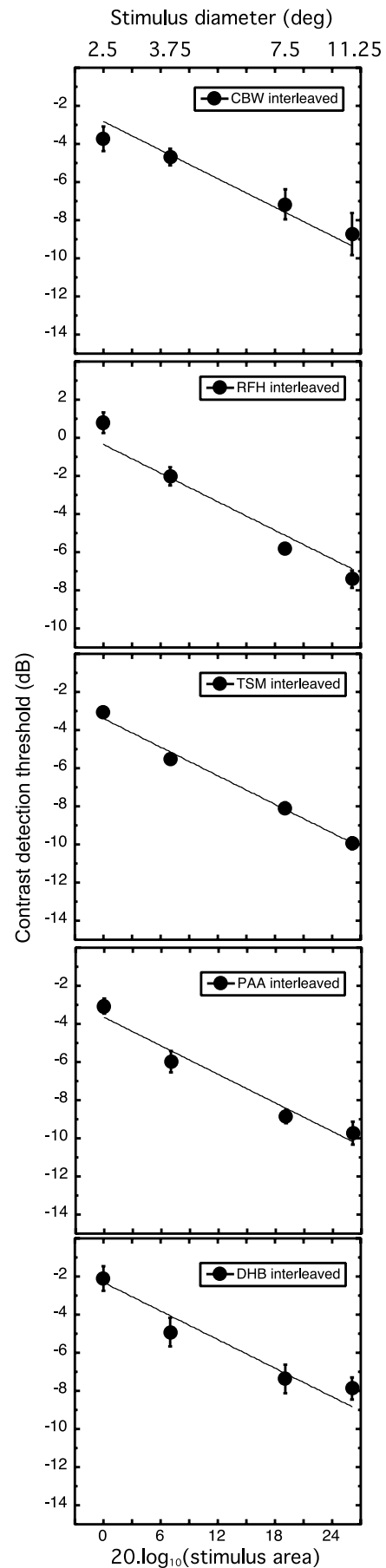
After 1997, but before 2001, our standard procedure (in the Aston laboratory) became to monitor the standard error of each threshold determined by probit analysis and to discard and rerun experimental sessions where the standard error was greater than 3 dB. This was done for the second and third experiments here, but not the first, which predated the procedure’s introduction.

## Results and discussion

### Experiment 1a: Interleaved detection

The results of the interleaved detection experiment are shown in Figure 2 for five observers. For all observers, performance improved consistently with an increase in stimulus area over the range tested. The solid curves

Figure 2. Contrast detection thresholds as a function of stimulus area for five observers (different panels). In this and other figures, the abscissa is expressed as 20 times the log of stimulus area to be consistent with the contrast units of the ordinate (i.e., on both axes an interval of six units represents a factor of two). The size scale is normalized to the area of the smallest stimulus. The solid curve is the best-fitting straight line with a log–log slope of  $-0.25$ , equivalent to a fourth-root summation rule. Error bars are  $\pm 1$  SE, where larger than symbol size. See Table 1 for best-fitting slopes.



Observer	Experiment type	Figure	Slope	Exponent
CBW	Interleaved	1	-0.194	5.15
RFH	Interleaved	1	-0.314	3.18
TSM	Interleaved	1	-0.255	3.92
PAA	Interleaved	1 and 3	-0.252	3.97
DHB	Interleaved	1 and 3	-0.217	4.61
TSM	Interleaved	3	-0.230	4.35
TSM	Blocked	3	-0.279	3.58
PAA	Blocked	3	-0.233	4.29
DHB	Blocked	3	-0.227	4.41
Mean	-	-	-0.244	4.10
SE	-	-	-0.012	0.17

Table 1. Log-log slopes of best-fitting straight lines to the detection data from Experiments 1a, b, and 2. The final column is the reciprocal of the absolute slope and equivalent to the best-fitting exponent in a Minkowski spatial pooling metric, assuming a linear contrast transducer.

are the best-fitting straight lines with a slope of  $-0.25$ , consistent with a fourth-root area summation rule, and provide good descriptions of the data. The slopes of best-fitting straight lines to each of these data sets are shown in Table 1 (see also Experiment 2). The average slope is very close to a fourth-root summation rule. We do note, however, that for two observers (PAA and DHB) there is a tendency for performance to level off at the larger stimulus size. This is broadly consistent with earlier findings where area summation has been found to apply for only limited spatial extent and is probably due to a general decline in contrast sensitivity away from the fovea (e.g., Howell & Hess, 1978; Robson & Graham, 1981; Rovamo et al., 1993).

### Experiment 1b: Interleaved discrimination

The results of the interleaved discrimination experiment are shown in Figure 3 for 11 observers (solid symbols are for the same five observers as in Figure 2). The discrimination thresholds have been normalized across observers to illustrate the trends. For completeness, the thresholds and standard errors for the smallest stimulus size for each observer are given in Table 2. Whereas the pattern of results for the detection experiment was consistent across observers, this is clearly not the case for the discrimination experiment. For some observers (e.g., TSM), there was little or no improvement in performance as stimulus size increased. For others (e.g., PAA), there was a clear improvement in performance with stimulus size, although in most cases performance tended to plateau or deteriorate again as stimulus size continued to increase. The solid grey curves show predictions for fourth-root and square-root summation rules. In some cases, summation was greater than the fourth-root

rule and closer to the square-root rule, at least for the initial part of the function (i.e., the left side of the plot).

Overall, there is a great deal of variation across observers, but the average performance (crossed square symbols) indicates that sensitivity is higher for the larger stimuli than for the smallest, showing that the overall variability is around a systematic trend. We confirmed these observations by performing a balanced ANOVA on a restricted set of the raw data<sup>1</sup> where replication was a random factor. The results were highly significant for the main effects of area ( $F_{3,135} = 41.7, p < .001$ ) and observer ( $F_{9,135} = 9.96, p < .001$ ), and the interaction between area and observer was also significant ( $F_{27,135} = 1.79, p = .016$ ).

### Experiment 2: Blocked and interleaved detection and discrimination

In the detection experiment above, the different size conditions were interleaved in an attempt to keep the spatial window of attention fixed so that this was not confounded with stimulus size (Graham, 1989; Tyler & Chen, 2000). It seemed reasonable to use the same design for the

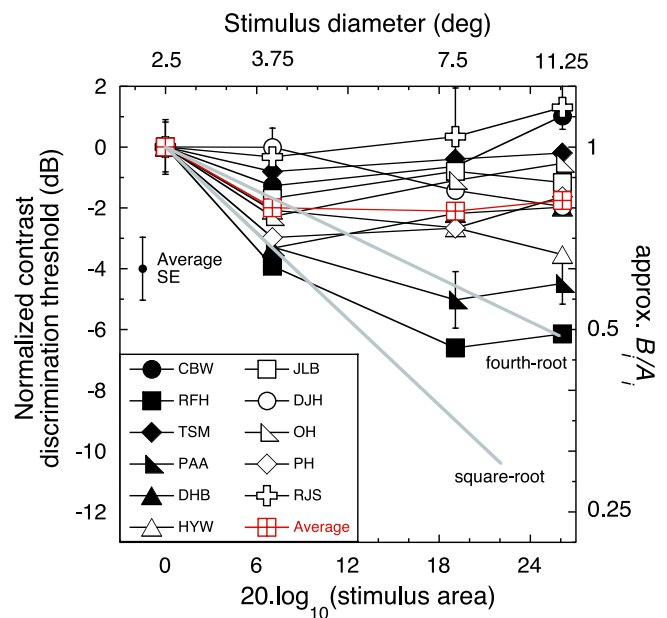


Figure 3. Contrast discrimination thresholds (pedestal contrast was 20%) as a function of stimulus area for 11 observers and their average. The discrimination thresholds have been normalized to 0 dB for the smallest stimulus size (see Table 2 for absolute discrimination thresholds). For clarity, error bars ( $\pm 1$  SE) are shown for two observers only (PAA and RJS). The average standard error is also shown. The grey curves are predictions for fourth-root and square-root (quadratic) summation rules. The dark curves are fits of the descriptive model (see text for details). The right-hand y-axis is explained in the model section of the text. Solid symbols denote the observers who took part in the detection experiment in Figure 2.

Observer	Detection		<i>n</i>	Discrimination		<i>n</i>
	threshold (dB)	SE (dB)		threshold (dB)	SE (dB)	
CBW	-3.74	0.64	4	12.88	1.89	6
RFH	0.78	0.54	4	11.27	0.62	6
TSM	-3.07	0.28	6	7.50	1.00	6
PAA	-3.10	0.40	4	12.00	0.82	8
DHB	-2.78	1.11	4	9.33	0.78	6
HYW	-	-	-	5.83	2.63	6
JLB	-	-	-	9.73	1.40	11
DJH	-	-	-	8.65	1.15	8
OH	-	-	-	11.14	1.10	8
PH	-	-	-	9.32	1.02	5
RJS	-	-	-	11.99	0.71	6

Table 2. Thresholds, standard errors, and number of replications for the smallest stimulus size. Detection thresholds are for the five observers in Figure 2 and discrimination thresholds are for the 11 observers in Figure 3. Note that the variation in detection thresholds is well within the range that might be expected from the model-fest observers (e.g., Watson, 2000).

discrimination experiment against which the detection data were to be compared. However, the situation is slightly different in the discrimination experiment because the clearly visible mask stimulus provides the observer with information about the size of the test stimulus on the first interval of each trial. It is not obvious how this might have affected the results, but it is possible that it prompted different strategies of attention across observers (see Results and discussion). To test whether this could be held responsible for the IDs in the discrimination data, the experiment was repeated using a blocked design on three observers, two of whom had shown summation for contrast discrimination (PAA and DHB) and one of whom had not (TSM). For completeness, these observers repeated the detection experiment also using a blocked design. For all three observers, the data for the two different experiments and the two different designs were gathered within a few days of each other (see Methods).

A comparison of the interleaved and blocked detection experiments is shown in Figure 4. All of these results are broadly consistent with a fourth-root summation rule (see Table 1 for best fits) and replicate the findings in Figure 2. The results for the discrimination task are shown in Figure 5 and replicate the main findings in Figure 3. Performance is little affected by area for TSM, but PAA and DHB both show improvement over the initial region of the functions. The curves in Figure 5 are the best fits of a fourth-root summation rule. Clearly, this rule is inadequate for all these discrimination data.

But the main point here is that blocking or interleaving trials for different stimulus sizes had no systematic effect on the results for either the detection task or the discrimination task. In other words, the IDs are replicable and robust to the choice of experimental design.

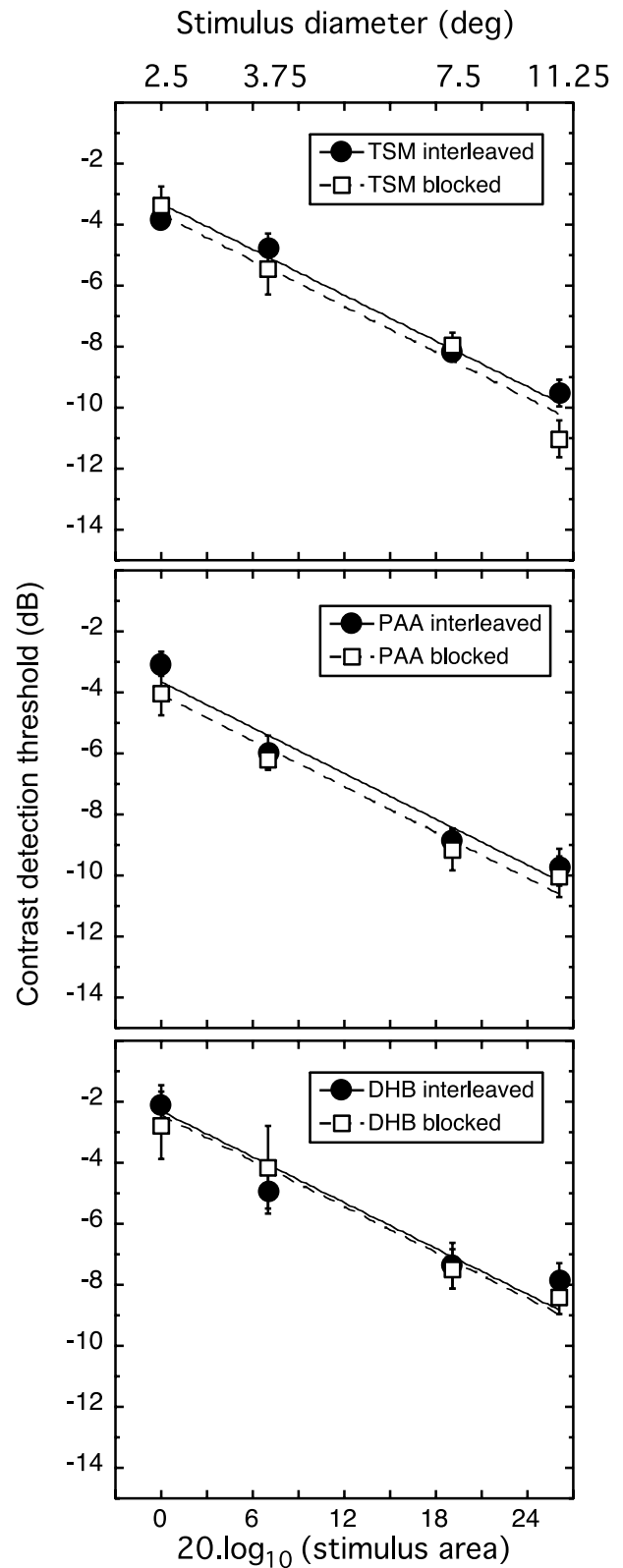


Figure 4. Contrast detection thresholds for three observers (different panels) for interleaved and blocked experimental designs (different symbols). The curves are the best-fitting straight lines with a log–log slope of  $-0.25$ . This summation rule provides a good description of these data. Error bars show  $\pm 1$  SE. For PAA and DHB, the interleaved data are replotted from Figure 2.

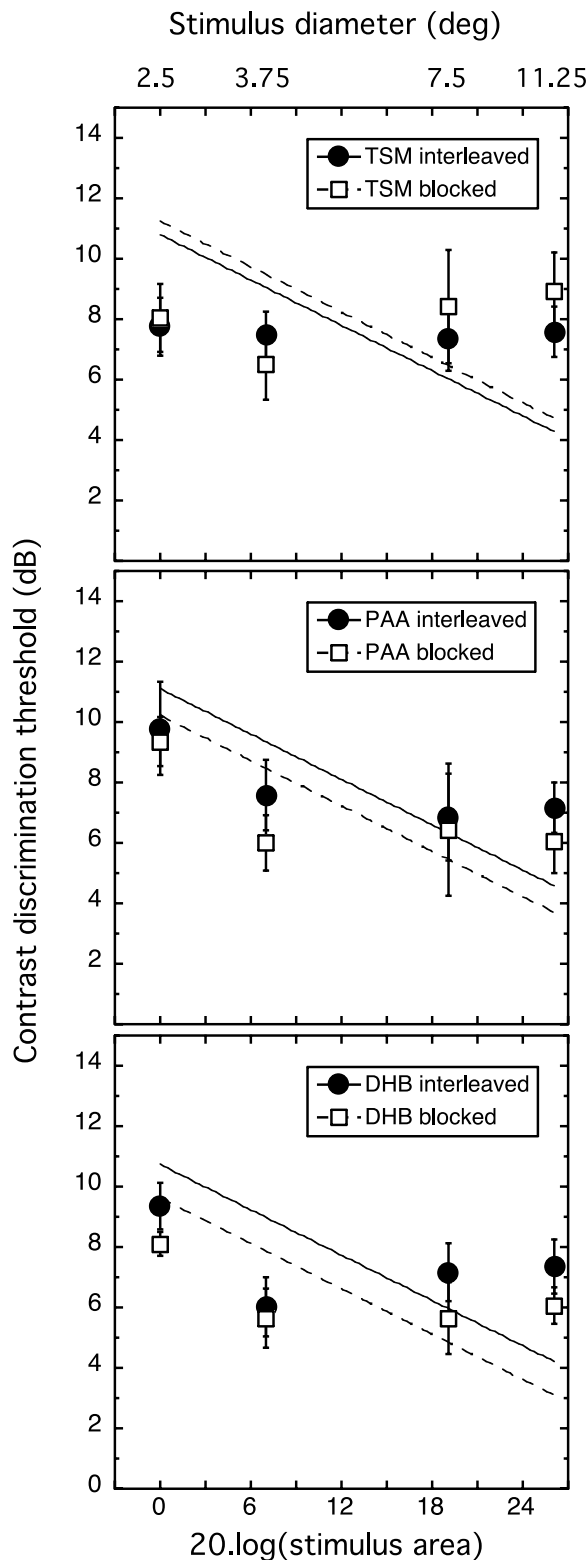


Figure 5. Contrast discrimination thresholds (pedestal contrast was 20%) for three observers (different panels) for interleaved and blocked experimental designs (different symbols). The curves are the best-fitting straight lines with a log–log slope of  $-0.25$ . This summation rule provides a poor description of these data. Error bars show  $\pm 1$  SE. For DHB, the interleaved data are replotted from Figure 2.

## Model preamble

In this section, we extend an earlier model of area summation (Meese, 2004) to accommodate the multiple stimulus sizes used here. After constraining the model to fit all the detection data and the discrimination threshold for the smallest stimulus size, we were left with three free parameters (three suppressive weights), which were adjusted to fit the relative levels of summation in Figure 3. As the number of free parameters equals the number of data points being fit for each observer, it is not surprising that the model performs so well (see Figure 3). However, the exercise allows us to make several points. First we are demonstrating that a widely used expression for contrast gain control (Foley, 1994) can be readily adapted to accommodate IDs in contrast discrimination data while at the same time describing a consistent pattern of results at detection threshold. Second, the analysis points to a possible locus of the IDs. Third, we show that on this interpretation, area summation data at and well above detection threshold deliver good approximations of different model parameters directly.

In the Appendix, we consider the relationship between the descriptive model developed here and several versions employing Minkowski summation.

## Area summation model

For the main experiments here, Equation 1 can be rewritten as follows:

$$\text{resp}_i(c) = \frac{\alpha_i c^p}{1 + \beta_i c^q}, \quad (2)$$

where  $\text{resp}_i$  is the contrast response of the visual system to the mask or mask plus test stimulus,  $c$  is stimulus contrast (in percent), the exponent  $p$  controls the rate of response acceleration at low stimulus contrasts, the exponent difference ( $p - q$ ) controls the rate of response compression at higher contrasts, and the coefficients  $\alpha_i$  and  $\beta_i$  control the weights of excitation and suppression for the four different stimulus sizes ( $i = 1$  to 4). Here, we find it convenient to express the weights as  $\hat{A}$  and  $\hat{B}$  for the smallest stimulus size ( $i = 1$ ) and use  $A_i$  and  $B_i$  to express the weights for the other stimulus sizes relative to those for  $i = 1$ . Thus,  $\alpha_i = \hat{A} \cdot A_i$ ,  $\beta_i = \hat{B} \cdot B_i$  and  $A_i = B_i = 1$ . As we shall see later, our conclusions do not require precise estimates of the linear scaling parameters  $\hat{A}$  and  $\hat{B}$ , and our interest is confined mainly to  $A_i$  and  $B_i$ . [Intuitively, this is because the interesting features of the data are not the IDs in absolute thresholds (e.g., see Table 2), but those differences that remain after normalization (i.e., the interaction between observer and area).]

Our data do not constrain the values of  $p$  and  $q$  so we set these to default values of 2.4 and 2, respectively (Legge & Foley, 1980). As we illustrate below, these

choices of  $p$  and  $q$  are not critical for our conclusions, although  $p$  should be a little larger than  $q$ . Instead, we might have simplified the model by omitting  $p$  and  $q$  from our analysis, but we prefer to include them for completeness and comparison with other work.

A stimulus is detected when

$$\text{respdiff}_i = \text{resp}_i(C + \Delta C) - \text{resp}_i(C) = 1, \tag{3}$$

where  $C + \Delta C = c$  for the mask + test stimulus, and  $C = c$  for the mask stimulus alone. This formulation is consistent with a limiting Gaussian noise source that is late and additive.

In the contrast detection task, Equation 2 reduces to

$$\text{resp}_i(c) \approx \hat{A} \cdot A_i c^p \tag{4}$$

because when mask contrast ( $C$ ) equals zero, the denominator of Equation 2 is dominated by the saturation constant of unity.<sup>2</sup>

From Equation 4, it is clear that with  $p$  already set to 2.4, the contrast at detection threshold (where  $\text{respdiff}_i = 1$ ) for the smallest stimulus size gives an estimate of  $\hat{A}$  because

$$\hat{A} \approx \frac{1}{\Delta C^p}. \tag{5}$$

Furthermore, from Equations 3 and 4,

$$A_i \approx \frac{1}{(\Delta C_i / \Delta C_1)^p}. \tag{6}$$

But from the curve fitting in Figures 3 and 5, we know that the detection data are well described by a fourth-root area summation rule, so we set

$$\Delta C_i / \Delta C_1 = (\text{area}_i / \text{area}_1)^{-1/4}, \tag{7}$$

where  $\text{area}_i$  is the area of the  $i$ th stimulus size. From Equations 6 and 7, we now have

$$A_i \approx (\text{area}_i / \text{area}_1)^{p/4}. \tag{8}$$

Thus, Equation 8 sets the slope of the area summation curve at threshold, and the vertical offset that provides the best fit of this curve to the data (e.g., see Figures 2 and 4) provides another way of estimating  $\hat{A}$ .

We now turn our attention to the contrast discrimination task. Equations 2 and 3 specify the model completely and were fit to the data in Figure 2, where the values of  $\beta_i$  were solved numerically. For the six observers for whom we did not measure detection thresholds, we assume that the fourth-root summation rule is a fair description of their sensitivity at threshold. We then created synthetic detection data for these observers (justified by the sim-

ulations described below) as follows. For the smallest stimulus size, the differences between the detection and discrimination thresholds were averaged from the five observers who performed both tasks (Figures 2 and 3). For each of the other observers, this value was subtracted from their discrimination threshold to give an estimate of detection threshold for the smallest stimulus. The remainder of the synthetic detection data was set according to a fourth-root summation rule.

The solid curves in Figure 3 are the fits of the model to the data. The values of  $\hat{A}$  and  $\hat{B}$  (not shown) are of little interest as they serve merely to offset the fits (i.e., to describe the main effect of observer by sliding the detection and discrimination fits vertically on log axes). However, the interaction between observer and size is described by  $B_i$ , whose values are revealed in an interesting way. Consider the following. In the discrimination task, Equation 2 reduces to

$$\text{resp}_i(c) \approx (\alpha_i / \beta_i) c^{(p-q)} \tag{9}$$

because the contrast term in the denominator of Equation 2 dominates the saturation constant.

Combining Equations 3 and 9, we have

$$(C + \Delta C_i)^{(p-q)} - C^{(p-q)} \approx \beta_i / \alpha_i. \tag{10}$$

For reasonable values of  $p$  and  $q$ , the left-hand side of Equation 10 is approximately linear with  $\Delta C$  over a reasonable range of contrast, as shown in Figure 6. This means

$$\frac{\Delta C_i}{\Delta C_1} \approx \frac{\beta_i / \alpha_i}{\beta_1 / \alpha_1}, \tag{11}$$

and therefore

$$\frac{\Delta C_i}{\Delta C_1} \approx \frac{B_i}{A_i}. \tag{12}$$

In other words, according to this model, the data in Figure 3, which plot  $20 \log_{10}(\Delta C_i / \Delta C_1)$ , provide a direct estimate of how the weight of suppression grows with area ( $B_i$ ) relative to the growing weight ( $A_i$ ) of excitation (right-hand ordinate of Figure 3).

Another view of these parameters is given in Figure 7, where  $A_i$  and  $B_i$  are plotted separately for each observer (only  $B_i$  differ across observers). Note that because this model is really just an alternative description of the data, it necessarily reflects the noise in our data as well as the parameters of interest. Nevertheless, a comparison of Figures 3 and 7 reveals a clear trend. In contrast discrimination, empirical area summation occurs if the suppressive weight  $B_i$  does not keep pace with the excitatory weight  $A_i$  as stimulus size increases. (Note that on the axes of Figure 7, the slope of  $A_i$  against area is given by  $p/4$ .)

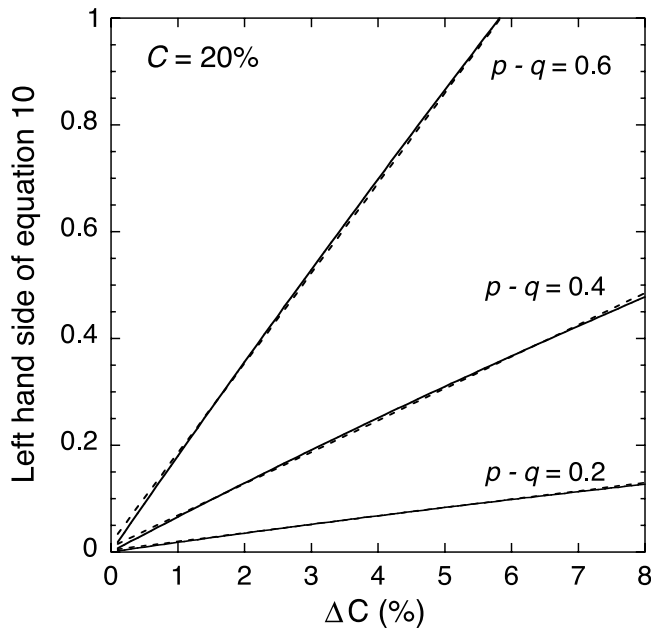


Figure 6. The left-hand side of Equation 10 is approximately a linear function of  $\Delta C$ . Solid curves show Equation 10 for three different values of  $p - q$ , and dashed curves are the best-fitting straight lines over the range  $\Delta C = 0$  to 8%.

In making the assertion above regarding the right-hand ordinate of Figure 3, we made several approximations. We justified all of these by extensive simulations in which we tried the following adjustments in fitting the full version of the model. We set detection threshold for the smallest stimulus to  $-6, -3, 0, 3,$  and  $+6$  dB relative to the estimate from the synthetic data described above for each observer. We then tried all possible combinations of the following model parameters, with each estimate of threshold:  $p = 2.4, p = 3, p - q = 0.3, p - q = 0.4, p - q = 0.5$ . This produced a total of 330 simulations. We found that deviations between the data  $\Delta C_i / \Delta C_1$  and the model parameter ratio  $B_i / A_i$  were typically negligible and rarely worse than 0.3 dB. Only for observers CBW and RJS did the deviations exceed 0.5 dB. Even then, this was for a limited set of parameter values and typically for only the data points where discrimination thresholds were worse than that for the smallest stimulus.

In sum, we have shown that each data point from Experiments 1a, b, and 2 carries a very good approximation to a direct quantitative interpretation within the context of a widely used model of contrast gain control. On this view, the IDs between observers provide a direct indication of different parameter values between observers.

### Experiment 3: Spatial inhomogeneity and lateral interactions for contrast discrimination

From Experiments 1a, b, and 2, it is clear that in a contrast discrimination task, increasing the size of the

stimulus confers no advantage for some observers (e.g., TSM) but does for others (e.g., RFH, DHB, and PAA). One possibility is that the gain in performance for the larger stimuli might be due to greater sensitivity to contrast increments in the outer stimulus regions. We tested this by performing a final experiment in which we measured contrast discrimination thresholds for a small stimulus patch (SS), a large stimulus patch (LL), and a doughnut stimulus (DD) constructed from the difference between the first two stimuli (see Methods). We also investigated two further configurations. In the Introduction section, we highlighted that IDs have been found for lateral interactions in a contrast-matching task (Cannon & Fullenkamp, 1993). On a much smaller sample of observers ( $n = 3$ ), Meese (2004) also found IDs for lateral interactions using a contrast discrimination task. But the models (and experiments) above do not determine whether the IDs seen here are due to IDs in size functions of surround interactions, self-suppression, or a combination of the two because for each stimulus size all the suppressive effects are described by a single generic suppression parameter  $B_i$ . To try and shed some light on this, we included conditions in which the pedestals were always large and the test stimulus was either a small central patch (SL) or the outer annular region of the stimulus (DL).

We gathered data from three observers using the blocked design. From the earlier experiments, it was known that two of the observers show area summation for

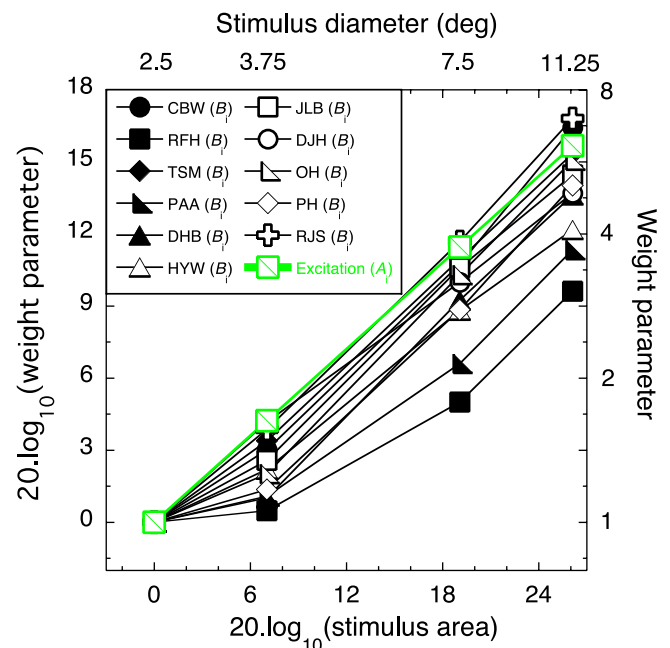


Figure 7. Suppressive weight parameter  $B_i$  for all observers. The excitatory parameter  $A_i$  was the same for all observers and is shown on the same axes with comparison (open green square with diagonal hash).

contrast discrimination (RFH and DHB) and one does not (TSM).

Normalized discrimination thresholds are shown in Figure 8 and reveal several points. A comparison of SS and LL shows that the earlier area summation results have been replicated for all three observers. A comparison of the SS and SL configurations reveal that the surround has no effect for TSM but causes a drop in performance for RFH and DHB. For TSM, this confirms a result from Meese (2004). A similar result can also be seen for the average observer in Yu, Klein, and Levi (2003). For the other two observers here (RFH and DHB), the influence of the surround was qualitatively similar to that shown by observer SK in the Meese (2004) study, JYS and KMF in Foley (1994), and JMF in Foley and Chen (1999).

Consider now, a comparison between the small (SS) and doughnut (DD) configurations. Just as we anticipated, RFH and DHB showed greater sensitivity to the DD configuration than the SS configuration, whereas TSM did not. This is consistent with the view that the advantage for the large (LL) configuration for RFH and DHB was due in part to a higher sensitivity to contrast increments in the surround region than in the center region. Broadly speaking, a similar pattern of results was also seen for the DL configuration. Overall, the qualitative pattern of results across stimulus configurations was similar for RFH and DHB (the area summation observers), who were different from TSM (the no area summation observer).

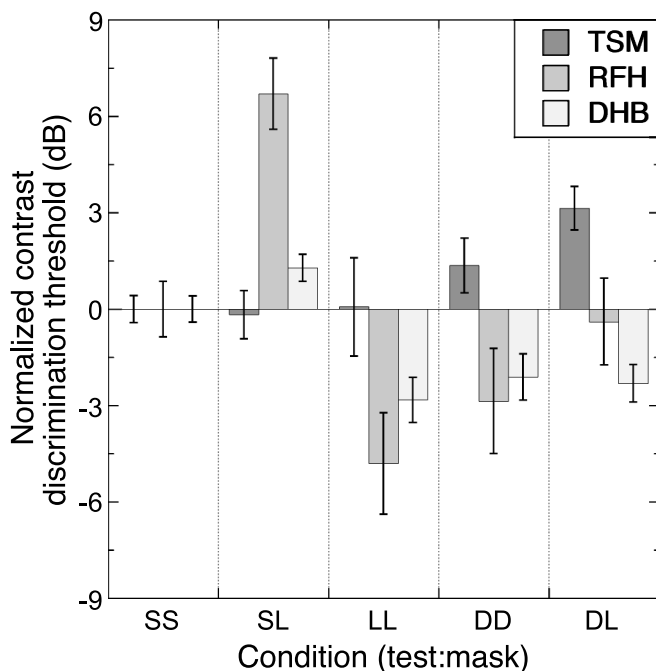


Figure 8. Normalized contrast discrimination thresholds for five different spatial configurations of test and mask stimuli (S = small, L = large, and D = doughnut). Pedestal contrast was 20%. Different shaded bars are for different observers. Error bars show  $\pm 1$  SEM of six replications.

In the remainder of this section, we consider how the results from Experiment 3 might be described within the context of the model we have been discussing. Readers concerned primarily with the main empirical results of this paper could skip to the General discussion without loss of continuity.

## Model overview

There are numerous model configurations that we might have constructed involving different assumptions about the number of detecting mechanisms and the nature of the lateral interactions, and the present data do little to guide or constrain these decisions. Nevertheless, we thought it natural to consider several variants of at least one simple model as follows. In our most general formulation, we suppose that the observer integrates signal and pedestal contrast over the signal region only, as suggested by Meese (2004), and according to a fourth-root rule. We also suppose that the denominator consists of three contrast terms. One of these is a self-suppressive term whose weight changes with stimulus size. In a ‘constrained’ version of the model, it remains proportional to the excitatory term (just as in Figure 1). In an ‘unconstrained’ version, it is multiplied by a single free parameter  $\gamma$ , when the size of the test is greater than S. The two other contrast terms control lateral interactions.

In one variant of our model, the lateral effects are additive (e.g., inhibitory) and in another variant they are subtractive (e.g., dis-inhibitory).

## Numerator terms and fixed parameters

The model exponents were fixed at  $p = 2.4$  and  $q = 2$  as before. The excitatory weights for the three different test stimuli were set according to Equation 8, where  $area_1 = 1$  for the small stimulus,  $area_3 = 9$  for the large stimulus, and  $area_2 = 8$  for the doughnut stimulus. The excitatory linear scaling parameter,  $\bar{A}$ , was set to 1. Specifically this gives

$$\begin{aligned}\alpha_1 &= 1, \\ \alpha_2 &= 8^{p/4}, \\ \alpha_3 &= 9^{p/4}.\end{aligned}$$

There were no free parameters for this part of the model.

## The unconstrained model

There were three contrast terms in the denominator of the gain control equation. They were self-suppression ( $\beta_i$ ), a lateral interaction from the center on a test in the

surround region ( $\beta_{cs}$ ), and a lateral interaction from the surround on a test in the center region ( $\beta_{sc}$ ). The weights  $\beta_{cs}$  and  $\beta_{sc}$  were free parameters in the model. The self-suppression term was set as follows:

$$\begin{aligned} \beta_1 &= \hat{B} \cdot \alpha_1, \\ \beta_2 &= \hat{B} \cdot \alpha_2 \cdot \gamma, \\ \beta_3 &= \hat{B} \cdot \alpha_3 \cdot \gamma, \end{aligned}$$

where  $\hat{B}$  and  $\gamma$  were free parameters in the model.

The contrast terms were combined to give the following model equation:

$$\text{resp}(c, i, c_c, c_s) = \frac{\alpha_i c^p}{1 + \beta_i c^q + \beta_{sc} c_s^p + \beta_{cs} c_c^q}, \quad (13)$$

where  $c_c$  and  $c_s$  were center and surround contrasts involved in the lateral interactions. These were determined by the stimulus configuration as shown in Table 3. The parameter  $c$  was the contrast in the test region and  $i$  was the index for the excitatory and self-suppressive weight parameters as described above (see Table 3). Strictly speaking, the saturation constant (set to unity in Equation 13) represented a degree of freedom for this experiment. But as we were dealing with high contrast stimuli (a pedestal contrast of 20%), its effect should be negligible, as it was here.

The model has four free parameters in total ( $\hat{B}, \gamma, \beta_{cs}$  and  $\beta_{sc}$ ).

### The constrained model

In a constrained version of the model, the number of free parameters was reduced to three by setting  $\gamma = 1$ . This tests the hypothesis that the observed differences in discrimination thresholds can be understood in terms of lateral interactions alone.

### Additive or subtractive lateral interactions in the contrast gain pool?

We tested two variants of the model for each version described above. In both variants, the term  $\beta_i$  was

	SS	SL	LL	DD	DL
$c$	$C + \Delta C$				
$i$	1	1	3	2	2
$C_c$	0	0	$C + \Delta C$	0	$C$
$C_s$	0	$C$	$C + \Delta C$	0	0

Table 3. Contrast and parameter assignments for the models and five stimulus configurations in Experiment 3.  $C$  is the pedestal contrast and  $\Delta C$  is the test contrast.

constrained to be  $\geq 0$ . In an additive variant, the terms  $\beta_{sc}$  and  $\beta_{cs}$  were also  $\geq 0$  and represent lateral suppression. In a subtractive variant, the terms  $\beta_{sc}$  and  $\beta_{cs}$  were  $\leq 0$  and represent lateral dis-inhibition, or contrast enhancement.

### Model fits

The models were fit to each of the three observers' data using a downhill simplex algorithm to minimize the RMS error of the fit (in decibels). The results for the constrained model described above (three free parameters) are shown in the top row of Figure 9 (see Table 4 for parameter values and RMS error). There are several points. For all observers, the subtractive variant provided better fits than the additive variant. For RFH and DHB, the additive variant clearly failed to describe the data, but the subtractive variant also has shortcomings. For RFH and DHB, it overestimates sensitivity to SS and underestimates sensitivity to LL to such an extent that, contrary to empirical observations, little or no area summation is predicted. This means that within the framework of the models considered here, the IDs cannot be understood in terms of different lateral interactions alone.

### Unconstrained model

In this model,  $\gamma$  was a free parameter meaning that the relation between self-suppression and area was not constrained to be the same as that between excitation and area. For TSM, the best-fitting value was close to unity (see Table 3), meaning that improvement in model performance was marginal. For RFH and DHB,  $\gamma$  was markedly less than unity, and the performance of both variants of the model improved substantially. For the additive variant, however, the model was unable to account for the degradation in performance produced by adding a surround (SS vs. SL for RFH and DHB). Even when fitting was restricted to the first three configurations (SS, SL, and LL), the additive version failed to distinguish between the SS and SL configurations for both RFH and DHB (not shown). This is because the attenuating effects of the surround require the surround suppression weight ( $\beta_{sc}$ ) to be relatively large [ $\beta_1 = 0.22$  and  $\beta_{sc} = 3.03$  for RFH and  $\beta_1 = 0.17$  and  $\beta_{sc} = 0.91$  for DHB, when fit to SS and SL alone (not shown)]. But this results in far too much suppression for the LL configuration, where the larger excitatory weight provides insufficient compensation in the model. In short, the additive version of Equation 13 simply cannot handle the magnitude of both of these effects (SS vs. SL and SS vs. LL) for either RFH or DHB.

It is noteworthy that the problem with the additive variant (see above) did not arise in the Meese (2004) study where a similar model was fit to dipper functions

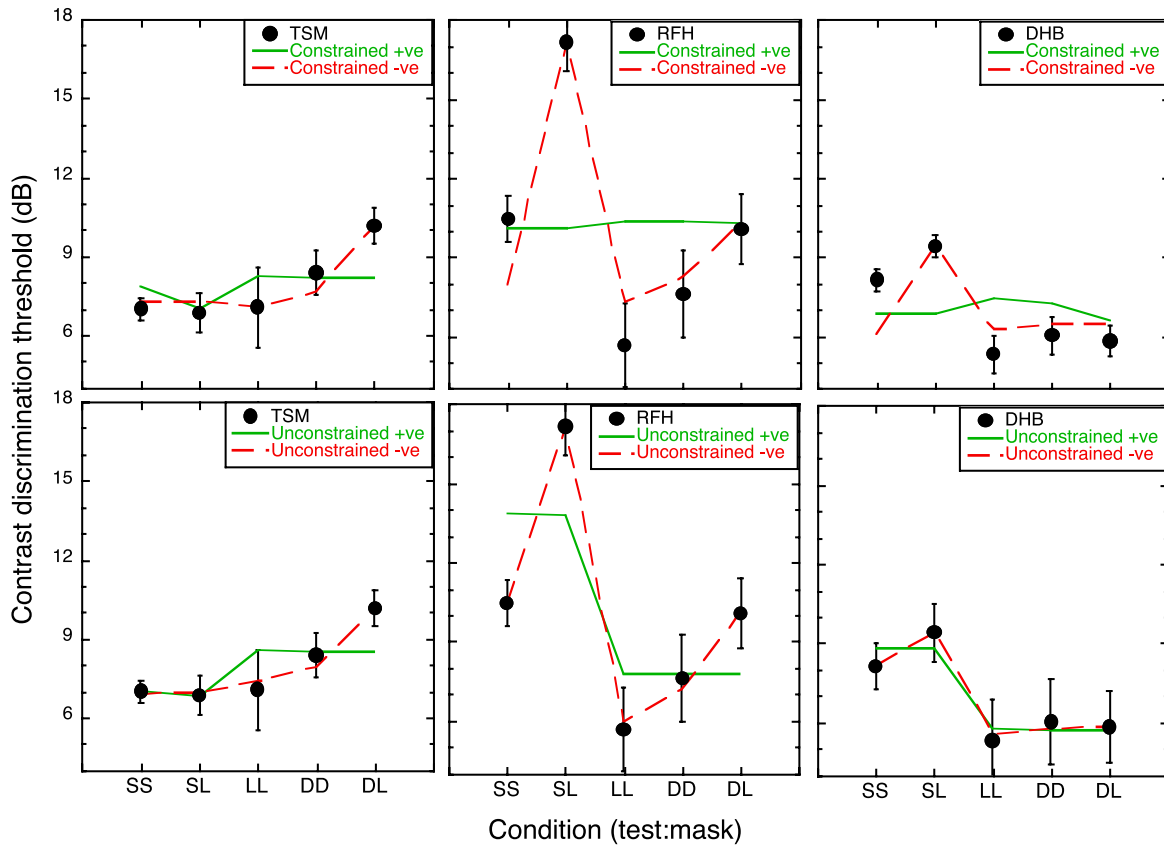


Figure 9. Contrast discrimination thresholds (replotted from Figure 8) for three observers (different columns) and four different model variants (different rows and different curves). The constrained and unconstrained model fits (3 and 4 free parameters, respectively) are shown in the top and bottom rows (see Table 4 for model parameters). Solid (green) curves are for the additive model variant and dashed (red) curves are for the subtractive model variant.

for configurations similar to some of those used here (SS, SL, and LL), although observer SK in that study was qualitatively similar to RFH and DHB here. [The parameters  $S_{wc}$ ,  $S_{ws}(SL)$ , and  $S_{ws}(LL)$  in model version

2B of that study are related to  $\beta_1$ ,  $\beta_{sc}$ , and  $(\beta_{sc} + \beta_3 - \beta_1)$ , respectively, in the present study.] Probably part of the reason for this difference is that the large–small area ratio was much greater in Meese (2004) than in Experiment 3

	Additive			Subtractive		
	TSM	RFH	DHB	TSM	RFH	DHB
<i>Constrained</i>						
RMS error (dB)	1.104	3.999	1.708	0.403	1.386	1.066
$\beta$	0.167	0.182	0.150	0.157	0.168	0.138
$\beta_{cs}$	0.000	0.001	0.011	-0.035	-0.032	-0.000
$\beta_{sc}$	0.006	0.664	0.000	-0.000	-0.029	-0.012
$\gamma$ (fixed)	1	1	1	1	1	1
<i>Unconstrained</i>						
RMS error (dB)	0.923	2.546	0.478	0.254	0.236	0.175
$\beta$	0.152	0.312	0.184	0.151	0.220	0.171
$\beta_{cs}$	0.000	0.000	0.001	-0.033	-0.037	-0.002
$\beta_{sc}$	0.001	0.000	0.000	-0.000	-0.031	-0.007
$\gamma$	1.137	0.511	0.694	1.075	0.681	0.745

Table 4. Free parameter values (to three decimal places) and goodness of fit for the four different model variants fit to the results from Experiment 3.

here (by a factor of 8.5), and substantial lateral suppression (for the SL configuration) could be compensated by the larger excitatory weight in the LL configuration in Meese (2004). The SS versus LL effect was also less for observer SK in that study than it was for RFH or DHB here.

Returning to the present work, for the subtractive variant of the unconstrained model, the model curves slid nicely into place (compare the dashed, red curves for the constrained and unconstrained models in Figure 9). However, with only one fewer free parameters than data points for each observer, the fits could be fortuitous, and while we feel confident in rejecting the additive models, at least for RFH, the unconstrained subtractive model must remain a tentative proposal until it receives further direct testing. Furthermore, it should be noted that the subtractive model variant was developed specifically for the high contrast stimuli used here. It is clear that further development would be required to handle stimuli that cause the denominator of Equation 13 to become very small (resulting in extremely high contrast responses) or negative, as could happen if the surround contrast was much higher than the center contrast (due to the negative contrast term).

Finally, we note that the subtractive variant describes the drop in performance produced by the surrounding mask (SS vs. SL) for RFH and DHB, although the surround diminishes the overall level of suppression for the SL configuration in the model (i.e., the model causes masking by contrast enhancement, not suppression). Similar counterintuitive model behaviors have been noted several times before (Bruce, Green, & Georgeson, 2003; Chen & Tyler, 2002; Meese, 2004; Yu, Klein, & Levi, 2003). It is noteworthy though that to achieve the same level of lateral masking (SS vs. SL), the strength of the interaction is very much weaker when it is negative than when it is positive (e.g., for RFH,  $\beta_{sc} = 3.03$  from the text above, or  $\beta_{sc} = -0.031$  from Table 4).

## General discussion

### Summary of main results and model

We have investigated area summation at and above detection threshold for 1 c/deg circular patches of grating with retinal field sizes between 2.5 and 11.25 degrees. At detection threshold, we confirmed the fourth-root summation-of-area rule that has been described many times before (e.g., see Graham, 1989). Previous work (Legge & Foley, 1980) found no summation of contrast when the test stimulus was placed upon a pedestal whose size was matched to the test, leading to the widespread view that area summation is abolished well above threshold (e.g., McIlhagga & Pääkkönen, 1999; Näsänen et al., 1998).

However, using a pedestal contrast of 20%, we found the pattern of results varied across 11 observers. Most observers showed little or no summation with area, but this was not universal. For some observers, summation was quite marked being even greater than that seen in the detection case. However, for no observer did the contrast discrimination data follow a fourth-root summation rule over the range of stimulus sizes in which it was seen in the detection experiment. These general observations did not depend upon whether the experiment used a blocked or interleaved design for stimulus area.

We describe all of the results in the context of a contrast gain control model. On this model, the pattern of excitatory weights across our range of stimulus sizes follows a fourth-root law for all observers tested (subject to log scaling by an accelerating nonlinearity,  $p$ ), describing the good approximation of this rule at detection threshold. However, the pattern of suppression in the model is much less similar across observers, and this describes the IDs seen in the discrimination data. For some observers, suppression grows with approximately the fourth-root of stimulus area (subject to the same scaling as the excitatory weight), in which case behavior in the discrimination task is as though there is little or no summation of contrast. However, for other observers, suppression grows more slowly than this, resulting in contrast summation behavior that can reach or exceed quadratic summation in the early part of the discrimination function.

### Alternative explanations and possible confounds

One question is whether the observer differences truly represent differences in sensory processes, or differences in strategy in the discrimination task. If the variation in discrimination thresholds is to be attributed to strategy, then it must be one that would lead some observers to perform least well for the smallest stimulus size. One possibility is that observers allocated their attention to stimulus regions away from the center of the display, compromising performance for the smallest stimulus. This is at least plausible in the interleaved design—perhaps the larger stimulus patches draw attention away from the center—but it seems very unlikely in the blocked design. In this case, one would have to argue that an observer's ability to attend to the center of the display was compromised in the smallest size condition, even when he or she knew that this would be the most appropriate strategy for a block of 100 or so trials. This is difficult to reconcile with conventional thinking in visual psychophysics.

Another way in which strategy might be important is if the contrast response to the large stimulus was not uniform. In this case, performance might depend upon which part of the stimulus contrast judgements were being

made. Clearly, we cannot rule out this possibility, but the fact remains that for some observers there was a region available in the large stimulus, which allowed performance to improve over that in the small stimulus, and this invokes a sensory process. Another possibility along similar lines is that multiple visual mechanisms are involved. For example, the large patch might be processed by multiple mechanisms with various sized regions of integration, suppression, and other lateral interactions. The observer is then faced with the problem of deciding which mechanisms to use for the task. Perhaps some observers (those that show area summation) are more adept at selecting the more efficient mechanisms for the larger stimuli, and that this is responsible for the IDs. In this case, [Equation 2](#) summarizes the net behavior of the entire process of sensation and mechanism selection.

Other issues regarding the IDs here concern psychophysical experience and learning/practice (e.g., Adini, Wilonsky, Haspel, Tsodyks, & Sagi, 2004; Yu, Klein, & Levi, 2004). The first of these factors is certainly not important for our results. TSM and RFH each have more than 16 years experience of psychophysical observations. Yet these two observers fall at the opposite extremes of our range, showing no and substantial area summation for contrast discrimination, respectively. We also think that task/stimulus-specific learning is unlikely to be important for our effect, at least in the medium term. TSM, RFH, DHB, and PAA each began the study with about 400 trials of practice on the main contrast discrimination task (using the interleaved design). Subsequently, TSM showed little or no area summation in the four out of four times he performed the task (see [Results and discussion](#)). However, RFH, DHB, and PAA showed the effect every time they were tested (twice, three, and three times, respectively). Of course, we cannot rule out the possibility that continued testing might cause a change in the behavior of one or more of these observers, but this does little to explain away our results.

Another potentially confounding factor worth considering is that of eye movements. Observers were instructed to fixate the center of the display, although we had no formal method of monitoring this. In principle, eye movements could move the stimulus away from the more sensitive region of the fovea and such an effect would be most severe for the smallest stimulus. So one possibility is that those observers who showed area summation for contrast discrimination were those who made eye movements in this task and compromised their sensitivity to the smallest stimulus. But (a) the detection data, which were consistent across observers, do not suggest a rapid decline in contrast sensitivity over the central region of the visual field (at 1 c/deg); so (b) the eye movements needed to produce the effect would have to be in the order of a few degrees and in any case frequent; and (c) of the three observers who showed the area effect several times (RFH, PAA, and DHB), all were well motivated, one was

highly experienced (RFH), another was psychophysically well-practiced throughout (PAA), and the other was psychophysically experienced by the time he performed [Experiment 3](#) (DHB). We think it unlikely that all three of these observers invalidated their data with frequent eye movements.

Another possibility is that the critical difference between the observers is some unknown factor that strongly correlates with suppression. For example, there is some evidence to suggest that lack of attention can enhance the effects of surround suppression (Zenger, Braun, & Koch, 2000) and that the presence of attention can enhance lateral facilitation (Shani & Sagi, 2005), although differences in task and stimulus design make comparisons with the present study problematic. Nevertheless, perhaps those observers who show lower levels of area summation for contrast discrimination were generally less attentive than the other observers. But even if there was an intermediate factor involved (such as attention), this would not undermine our analysis, which simply describes the latter part of this process (the differences in suppression).

## Individual differences

Our main empirical finding is that for some observers, contrast discrimination is not invariant with stimulus size (for a pedestal contrast of 20%). This contrasts with the study of Legge and Foley (1980), which is widely cited as showing no area summation for contrast discrimination. Legge and Foley measured dipper functions for 2 c/deg horizontal strips of grating with heights of 6 degrees and widths of 0.75 and 6 degrees. Their data were presented as the average of three observers (see [Figure 1](#)) and show area summation for low contrast pedestals, but an absence of area summation at higher contrasts. This general observation was confirmed on two other observers (TSM and PN) by Meese (2004) for 1 c/deg circular grating patches with diameters of 2 and 17.5 degrees, and for the average of two observers by Chirimuuta and Tolhurst (2005) who used a 2.7 c/deg Gabor patch and a grating. It is plausible that these observers had an arrangement of visual parameters similar to that of TSM, for whom it was shown again here that stimulus size has little or no effect in the contrast discrimination task. Close inspection of the data from the third observer (SK) from the Meese study, on the other hand, does show a small amount of summation (in the order of 2 dB) in the upper region of the dipper function (at and above a mask contrast of 8%, or 18 dB), consistent with the average level of summation seen here.

In another study, Bonnef and Sagi (1999) performed contrast discrimination for circular patches of 12.5 c/deg gratings presented with their centers 2.4 degrees into the periphery. Direct comparisons with the main experiments

from the present study are complicated by the facts that different spatial frequencies were used and different regions of the retina were stimulated as a function of area. However, Bonnef and Sagi's contrast discrimination functions were not flat functions of stimulus area (deviations were in the order of 3 dB) and they differed across their two observers (see the circle symbols in their Figure 2). It is difficult to judge whether these variations can be attributed solely to measurement error, but they are not inconsistent with the notion of IDs in suppression.

In a further study, Meese et al. (2001) compared contrast discrimination thresholds for stimuli containing single and multiple (177) Gabor patches with various spatial configurations (spatial frequency was 6.2 c/deg). For all three observers (TSM, CBW, and RFH), they found that performance was better in the multiple patch condition. But—and especially when only the results from the co-oriented condition of Meese and Holmes (2002) are considered—the number effect was most substantial for RFH (10.6 dB), smallest for TSM (2.4 dB), and intermediate for CBW (4.1 dB). This is a similar pattern of IDs seen for the same three observers in the current study (see Figure 3).

As mentioned in the Introduction, there are several instances in which IDs have been found for surround suppression when the surrounding mask and central test patch have the same spatial frequency and orientation. In a contrast-matching task, Cannon and Fullenkamp (1991b) found that the effect of suppression from a surround mask was consistently less (by about 3 dB) for one of their observers than the other two, but only when the mask was close to the test (see their Figure 5). Yu et al. (2001) also found IDs in surround suppression in contrast matches across their four observers (see their Figure 2a) using a spatial frequency of 8 c/deg. When the surround contrast was four times the center contrast, the differences between observers were as much as 6 dB. Cannon and Fullenkamp (1993) carried out a study designed specifically to address IDs in surround effects on contrast matching. Of particular note here, they found large differences across 10 observers (in the order of  $\pm 6$  dB) when the surround and center regions were of the same contrast (e.g., compare the 1X panels for observers MM, MS, and DR in their Figures 3, 4, and 6). Most of the Cannon and Fullenkamp study was conducted using a spatial frequency of 8 c/deg, but IDs were also found for two observers at 2 c/deg.

## Sensory accounts

In the model above, IDs were ascribed to different weights of suppression ( $B_i$ ), but could variations in other model parameters be responsible? The model parameters on the numerator of Equation 2 are set by the detection data, which leaves only the possibility that the exponent  $q$  varies with stimulus size. This is not easily dismissed, and a conservative position would state that the IDs in contrast

discrimination are due to IDs in suppression, arising from variations across  $B_i$  and/or  $q_i$ . But one consequence of attributing the effects to  $q$  is that the exponent difference ( $p - q$ ) would also vary with stimulus size and this predicts that the dipper handles of contrast masking functions should vary with stimulus size. The present data do not address this, but we know of no evidence to suggest it is so. Indeed, in the Meese (2004) study, IDs in contrast masking functions were consistent with different patterns in the parameter referred to here as  $B_i$ .

One natural interpretation of the suppression process we have been discussing is inhibition. However, Legge and Foley (1980) took a very different view. They attributed area summation at threshold to probability summation among independent detecting mechanisms (see Appendix) and the loss of summation above threshold to a loss of independence due to correlated noise. Our results do not discount this possibility and could be reinterpreted as IDs in the extent to which noise becomes correlated above threshold.

Yet another possible interpretation of  $B_i$  is that it does not interfere with the signal to noise ratio by changing the signal level (through suppression), but achieves an equivalent outcome (for detection and discrimination) by changing the noise level. If noise is more severe at higher contrasts, as would be the case if there were a multiplicative noise component (see Chirimuuta & Tolhurst, 2005; McIlhagga & Pääkkönen, 1999), then IDs in  $B_i$  might reflect individual variations of noise with stimulus size.

## Minkowski summation

Our gain control model of summation includes a weighting factor ( $\alpha_i$ ) applied to the excitatory contrast term as a function of stimulus size ( $i$ ). Another form of summation, widely used in the spatial vision literature, is Minkowski summation, where summation over  $j = 1$  to  $n$  variables ( $v$ ) is achieved as follows:

$$\text{Minkowski}_{\text{sum}} = \left( \sum_j |v_j|^k \right)^{1/k}, \quad (14)$$

where  $k$  controls the form of summation. It is possible to recast the present model this way, where Minkowski summation across area (Graham, 1989; Meese & Williams, 2000; Robson & Graham, 1981), replaces our area summation parameter  $\alpha_i$ , and the free parameters are recalculated for subscript  $j$  (different stimulus regions) instead of subscript  $i$  (different stimulus sizes). But what part of the model should be equated with  $v_j$  in Equation 14? In the Appendix, we show that equating  $v_j$  with  $c^p$  is identical to the current model when the Minkowski exponent  $k = 4/p$ . We also show that equating  $v_j$  with either  $\text{resp}$  or  $\text{resp}_{\text{diff}}$  is plausible.

## Conclusions

Consistent with much previous work, we find that a fourth-root summation rule provides a good description of area summation at contrast detection threshold for 1 c/deg patches of grating. This provides a direct indication of the weight of excitation subject to scaling (on log axes) by an excitatory response exponent  $p$ . Also consistent with earlier conclusions, we find that the fourth-root summation rule does not extend to contrast discrimination. However, we do find a highly significant size effect for contrast discrimination across our group of 11 observers. This has probably been missed in previous studies because contrast discrimination data (including ours) tend to be noisy, the average effect is small (about a factor of 1.25, or 2 dB), and the effect is not present for all observers. While we cannot rule out nonsensory (e.g., strategy based) explanations of our data, there is nothing that directs us to this interpretation. Instead, we describe the effects in terms of a contrast gain control equation. On this view, the area summation function for contrast discrimination does not reveal the excitatory summation process but provides information about a suppressive process. For all observers, the weight of suppression grows with stimulus size, but for many it does not keep pace with the weight of excitation. The IDs seen in this study suggest that suppression not only varies with stimulus size but also across observers.

## Appendix

Here we consider the relation between the model used in the main body of the paper and various model formulations using Minkowski summation. The purpose is to show that our own descriptive model, which uses excitatory weights indexed by area ( $A_i$ ), is largely consistent with other formulations where summation is achieved using a Minkowski metric. We do this by replacing  $A_i$  with Minkowski summation (in three different ways) and show that the models are either identical (for detection) or very similar (for discrimination).

The stimulus response for the model used in this paper is Equation 2, which is repeated here for clarity:

$$\text{resp}_i(c) = \frac{\alpha_i c^p}{1 + \beta_i c^q}, \quad (\text{A1})$$

where  $i$  is the index for stimulus size (here,  $i = 1$  to 4).

We also repeat that Minkowski summation of  $j = 1$  to  $n$  variables ( $v$ ) is achieved as follows:

$$\text{Minkowski}_{\text{sum}} = \left( \sum_j |v_j|^k \right)^{1/k}, \quad (\text{A2})$$

where  $k$  controls the form of summation.

## Minkowski summation of a single interval response

From the main body of the paper, Equation A1 can be rewritten as

$$\text{resp}_i(c) = \frac{\hat{A} A_i c^p}{1 + \beta_i c^q}. \quad (\text{A3})$$

Eradicating  $A_i$  and applying Minkowski summation to the response to a single stimulus interval, we have

$$\text{resp}_i(c) = \left[ \sum_{j \in \text{area}_i} \left| \frac{\hat{A} c^p}{1 + \lambda_j c^q} \right|^k \right]^{1/k}, \quad (\text{A4})$$

where  $j$  is the elementary unit of size,  $\text{area}_i$  is the  $i$ th stimulus size, and  $\lambda_j$  replaces  $\beta_j$ . This gives us an alternative formulation against which to compare our own model.

### Contrast detection

For contrast detection, we use the same approximation as in the main body of the paper. Thus, Equation A4 becomes

$$\text{resp}_i(c) \approx \hat{A} \left[ \sum_{j \in \text{area}_i} c^{kp} \right]^{1/k}. \quad (\text{A5})$$

This can be rewritten as

$$\text{resp}_i(c) \approx \hat{A} \frac{\text{area}_i^{1/k}}{\text{area}_i} c^p. \quad (\text{A6})$$

This is the same as the model in the main body of the paper (Equations 4 and 8), when  $k = 4/p$ .

### Contrast discrimination

For contrast discrimination, we use the same approximation as in the main body of the paper. Thus, Equation A4 becomes

$$\text{resp}_i(c) \approx \hat{A} \left[ \sum_{j \in \text{area}_i} \left( \frac{c^{k(p-q)}}{|\lambda_j|^k} \right) \right]^{1/k}. \quad (\text{A7})$$

This can be rewritten as

$$\text{resp}_i(c) \approx \hat{A} c^{(p-q)} \left[ \sum_{j \in \text{area}_i} |\lambda_j|^{-k} \right]^{1/k}, \quad (\text{A8})$$

which is the same as

$$\text{resp}_i(c) \approx \hat{A} c^{(p-q)} \lambda'_i, \quad (\text{A9})$$

where

$$\lambda'_i = \left[ \sum_{j \in \text{area}_i} |\lambda_j|^{-k} \right]^{1/k}. \tag{A10}$$

Thus, a comparison of [Equations A9](#) and [9](#) (in the main body of the paper) shows that the two formulations are the same when

$$\lambda'_i = \frac{A_i}{\beta_i}. \tag{A11}$$

This is equivalent to saying

$$\frac{1}{\hat{B}\lambda'_i} = \frac{B_i}{A_i}. \tag{A12}$$

[Equation A10](#) cannot decrease as a function of  $i$ , which means that the left-hand side of [Equation A12](#) can never be an increasing function of  $i$ . This is at odds with the right-hand side of [Equation A12](#), which from [Figure 3](#) (right-hand ordinate) does increase slightly for some observers over some regions of the function. However, the discrepancies are minor, and simulations with this version of the model (not shown) produce good fits to the data suggesting that this is a viable formulation of the model.

Another possibility is to lift the restriction that the sign of  $\lambda_i$  is not preserved. By rewriting  $|\lambda_i|$  as  $\text{sign}(\lambda_i)|\lambda_i|$ , where  $\text{sign}(\lambda_i) = 1$  if  $\lambda_i \geq 0$ , and  $\text{sign}(\lambda_i) = -1$  if  $\lambda_i < 0$ , then [Equation A9](#) can fit the data exactly. As this formulation implies negative contributions in the summation process, it violates the conventional interpretation of Minkowski summation in terms of nonlinear summation among independent neural responses, which are always positive. However, it could survive as an abstract description of the consequences of nonlinear suppressive interactions between the elementary units in question.

### Minkowski summation of response difference

In this formulation, Minkowski summation is applied to the response difference between the mask and mask + test intervals (e.g., [Watson & Solomon, 1997](#)). From ([Equations 2, 3, and A2](#)), we proceed as before by replacing  $A_i$  with the Minkowski sum to give

$$\left[ \sum_{j \in \text{area}_i} \left| \frac{\hat{A}(C + \Delta C)^p}{1 + \lambda_j(C + \Delta C)^q} - \frac{\hat{A}C^p}{1 + \lambda_j C^q} \right|^k \right]^{1/k} = 1, \tag{A13}$$

which is another formulation we wish to compare to our own.

### Contrast detection

For contrast detection,  $C = 0$  and  $\Delta C = c$ . Therefore, using the same approximation as before, [Equation A13](#) reduces to

$$\hat{A} \left[ \sum_{j \in \text{area}_i} c^{kp} \right]^{1/k} \approx 1. \tag{A14}$$

This is the same as [Equation A5](#), with  $\text{resp}_{\text{stim}} = 1$ , and therefore extends the earlier proof to the formulation considered here.

### Contrast discrimination

Using the same approximation for contrast discrimination as before, [Equation A13](#) becomes

$$\hat{A} \left[ \sum_{j \in \text{area}_i} \left| \frac{(C + \Delta C)^{p-q} - C^{p-q}}{\lambda_j} \right|^k \right]^{1/k} \approx 1, \tag{A15}$$

which simplifies to

$$\hat{A}[(C + \Delta C)^{p-q} - C^{p-q}] \left[ \sum_{j \in \text{area}_i} |\lambda_j|^{-k} \right]^{1/k} \approx 1, \tag{A16}$$

which rearranges to

$$\hat{A}(C + \Delta C)^{p-q} \left[ \sum_{j \in \text{area}_i} |\lambda_j|^{-k} \right]^{1/k} - \hat{A}C^{p-q} \left[ \sum_{j \in \text{area}_i} |\lambda_j|^{-k} \right]^{1/k} \approx 1. \tag{A17}$$

Both parts of the left-hand side of [Equation A17](#) have the same form as [Equation A8](#), which extends the previous proof to the formulation considered here with the same caveat as before.

### Minkowski summation of numerator response

In this novel formulation,  $A_i$  is replaced by Minkowski summation of the contrast term on the numerator of [Equation A3](#). With  $k = 4/p$ , this preserves the fourth-root summation behavior of the numerator ([Equation 8](#)) and leaves the rest of the model intact. It is therefore identical to the model in the main body of this paper.

## Acknowledgments

Financial support in Canada was from the Natural Science and Engineering Research Council (OGPOO

46528) and Medical Research Council (MOP-53346) awarded to RH. Financial support in the UK was from The Leverhulme Trust (F/00250/A) and The Wellcome Trust (069881/Z/02/Z) awarded to TM, and the Engineering and Physical Sciences Research Council (GR/S74515/01) awarded to TM and Mark Georgeson. We thank David Holmes for gathering data from some of the naïve observers and Mark Georgeson for helpful comments on an earlier draft.

Commercial relationships: none.

Corresponding author: Tim S. Meese.

Email: t.s.meese@aston.ac.uk.

Address: Vision Sciences, Aston University, Aston Triangle, Birmingham B4 7ET, UK.

## Footnotes

<sup>1</sup>To perform a balanced ANOVA, it was necessary to omit some of our data from the analysis. Most observers performed at least six replications of each condition (see Table 2). Therefore, we were able to include the last six thresholds measured for 10 of our 11 observers in the analysis. This resulted in 64 of the 304 estimates of contrast discrimination threshold being omitted. Most of the omitted data were from two observers (JLB and PH).

<sup>2</sup>We justified this simplification by comparing fits of the simplified model (Equation 4) with the full model (Equation 2) to the detection data, where the values of  $\beta_i$  in the full model were set by the discrimination data, and the values of  $A_i$  were constrained as described below. The differences in the fits of the two versions of the model were negligible (e.g., in Figure 2, deviations were between  $-0.13$  and  $0.15$  dB for RFH and even less for TSM).

## References

- Adini, Y., Wilonsky, A., Haspel, R., Tsodyks, M., & Sagi, D. (2004). Perceptual learning in contrast discrimination: The effect of contrast uncertainty. *Journal of Vision*, 4(12), 993–1005, <http://journalofvision.org/4/12/2/>, doi:10.1167/4.12.2. [PubMed] [Article]
- Bonneh, Y., & Sagi, D. (1998). Effects of spatial configuration on contrast detection. *Vision Research*, 38, 3541–3553. [PubMed]
- Bonneh, Y., & Sagi, D. (1999). Contrast integration across space. *Vision Research*, 39, 2597–2602. [PubMed]
- Bruce, V., Green, P. R., & Georgeson, M. A. (2003). *Visual perception: Physiology, psychology and ecology* (4th ed.). Psychology Press: Hove.
- Cannon, M. W. (1995). A multiple spatial filter model for suprathreshold contrast perception. In E. Peli (Ed.), *Vision models for target detection and recognition*. London: World Scientific.
- Cannon, M. W., & Fullenkamp, S. C. (1991a). A transducer model for contrast perception. *Vision Research*, 31, 983–998. [PubMed]
- Cannon, M. W., & Fullenkamp, S. C. (1991b). Spatial interactions in apparent contrast: Inhibitory effects among grating patterns of different spatial frequencies, spatial positions and orientations. *Vision Research*, 31, 1985–1998. [PubMed]
- Cannon, M. W., & Fullenkamp, S. C. (1993). Spatial interactions in apparent contrast: Individual differences in enhancement and suppression effects. *Vision Research*, 33, 1685–1695. [PubMed]
- Chen, C.-C., & Tyler, C. W. (2002). Lateral modulation of contrast discrimination: Flanker orientation effects. *Journal of Vision*, 2(6), 520–530, <http://journalofvision.org/2/6/8/>, doi:10.1167/2.6.8. [PubMed] [Article]
- Chirimuuta, M., & Tolhurst, D. J. (2005). Does a Bayesian model of V1 contrast coding offer a neurophysiological account of human contrast discrimination? *Vision Research*, 45, 2943–2959. [PubMed]
- Cornsweet, T. N. (1962). The staircase-method in psychophysics. *American Journal of Psychology*, 75, 485–491. [PubMed]
- Ejima, Y., & Takahashi, S. (1985). Apparent contrast of a sinusoidal grating in the simultaneous presence of peripheral gratings. *Vision Research*, 25, 1223–1232. [PubMed]
- Finney, D. J. (1971). *Probit analysis* (3rd ed.). Cambridge University Press: London.
- Foley, J. M. (1994). Human luminance pattern vision mechanisms: Masking experiments require a new model. *Journal of the Optical Society of America. A*, 11, 1710–1719. [PubMed]
- Foley, J. M., & Chen, C.-C. (1999). Pattern detection in the presence of maskers that differ in spatial phase and temporal offset: Threshold measurements and a model. *Vision Research*, 39, 3855–3872. [PubMed]
- Graham, N. (1989). *Visual pattern analyzers*. Oxford University Press: Oxford.
- Holmes, D. J., & Meese, T. S. (2004). Grating and plaid masks indicate linear summation in a contrast gain pool. *Journal of Vision*, 4(12), 1080–1089, <http://journalofvision.org/4/12/7/>, doi:10.1167/4.12.7. [PubMed] [Article]

- Howell, E. R., & Hess, R. F. (1978). The functional area for summation to threshold for sinusoidal gratings. *Vision Research*, *18*, 369–374. [PubMed]
- Laming, D. (1988). Precis of sensory analysis. *Behavioural and Brain Sciences*, *11*, 275–339.
- Legge, G. E., & Foley, J. M. (1980). Contrast masking in human vision. *Journal of the Optical Society of America*, *70*, 1458–1471. [PubMed]
- Luntinen, O., Rovamo, J., & Näsänen, R. (1995). Modelling the increase of contrast sensitivity with grating area and exposure time. *Vision Research*, *35*, 2339–2346. [PubMed]
- Manahilov, V., Simpson, W. A., & McCulloch, D. L. (2001). Spatial summation of peripheral Gabor patches. *Journal of the Optical Society of America A*, *18*, 273–282. [PubMed]
- McIlhagga, W., & Pääkkönen, A. (1999). Noisy templates explain area summation. *Vision Research*, *39*, 367–372. [PubMed]
- Meese, T. S. (1995). Using the standard staircase to measure the point of subjective equality: A guide based on computer simulations. *Perception & Psychophysics*, *57*, 267–281. [PubMed]
- Meese, T. S. (2004). Area summation and masking. *Journal of Vision*, *4*(10), 930–943, <http://journalofvision.org/4/10/8/>, doi:10.1167/4.10.8. [PubMed] [Article]
- Meese, T. S., Hess, R. F., & Williams, C. B. (2001). Spatial coherence does not affect contrast discrimination for multiple Gabor stimuli. *Perception*, *30*, 1411–1422. [PubMed]
- Meese, T. S., & Holmes, D. J. (2002). Adaptation and gain pool summation: Alternative models and masking data. *Vision Research*, *42*, 1113–1125. [PubMed]
- Meese, T. S., & Williams, C. B. (2000). Probability summation for detecting multiple patches of luminance modulation. *Vision Research*, *40*, 2101–2113. [PubMed]
- Näsänen, R., Tiippana, K., & Rovamo, J. (1998). Contrast restoration model for contrast matching of cosine gratings of various spatial frequencies and areas. *Ophthalmic and Physiological Optics*, *18*, 269–278. [PubMed]
- Olzak, L. A., & Laurinen, P. I. (1999). Multiple gain control processes in contrast–contrast phenomena. *Vision Research*, *39*, 3983–3987. [PubMed]
- Pelli, D. G. (1987). On the relation between summation and facilitation. *Vision Research*, *27*, 119–123. [PubMed]
- Petrov, Y., Carandini, M., & McKee, S. (2005). Two distinct mechanisms of suppression in human vision. *Journal of Neuroscience*, *25*, 8704–8707. [PubMed]
- Polat, U., & Norcia, A. M. (1998). Elongated physiological summation pools in the human visual cortex. *Vision Research*, *38*, 3735–3741. [PubMed]
- Polat, U., & Tyler, C. W. (1999). What pattern the eye sees best. *Vision Research*, *39*, 887–895. [PubMed]
- Robson, J. G., & Graham, N. (1981). Probability summation and regional variation in contrast sensitivity across the visual field. *Vision Research*, *21*, 409–418. [PubMed]
- Rovamo, J., Luntinen, O., & Näsänen, R. (1993). Modelling the dependence of contrast sensitivity on grating area and spatial frequency. *Vision Research*, *33*, 2773–2788. [PubMed]
- Rovamo, J., Luntinen, O., & Näsänen, R. (1994). Modelling contrast sensitivity as a function of retinal luminance and grating area. *Vision Research*, *34*, 1301–1314. [PubMed]
- Shani, R., & Sagi, D. (2005). Eccentricity effects on lateral interactions. *Vision Research*, *45*, 2009–2024. [PubMed]
- Swanson, W. H., Wilson, H. R., & Giese, S. C. (1984). Contrast matching data predicted from contrast increment thresholds. *Vision Research*, *24*, 63–75. [PubMed]
- Snowden, R. J., & Hammett, S. T. (1998). The effects of surround contrast on contrast thresholds, perceived contrast, and contrast discrimination. *Vision Research*, *38*, 1935–1945. [PubMed]
- Tyler, C. W., & Chen, C.-C. (2000). Signal detection theory in the 2AFC paradigm: Attention, channel uncertainty and probability summation. *Vision Research*, *40*, 3121–3144. [PubMed]
- Watson, A. B. (2000). Visual detection of spatial contrast patterns: Evaluation of five simple models. *Optics Express*, *6*, 12–33. [PubMed] [Article]
- Watson, A. B., & Solomon, J. A. (1997). A model of visual contrast gain control and pattern masking. *Journal of the Optical Society of America*, *14*, 2379–2391. [PubMed] [Article]
- Wetherill, G. B., & Levitt, H. (1965). Sequential estimation of points on a psychometric function. *British Journal of Mathematical & Statistical Psychology*, *18*, 1–10. [PubMed]
- Williams, A. L., Singh, K. D., & Smith, A. T. (2003). Surround modulation measured with functional MRI in the human visual cortex. *Journal of Neurophysiology*, *89*, 525–533. [PubMed] [Article]
- Wilson, H. R. (1980). A transducer function for threshold and suprathreshold human vision. *Biological Cybernetics*, *38*, 171–178. [PubMed]

- Xing, J., & Heeger, D. J. (2000). Center-surround interactions in foveal and peripheral vision. *Vision Research*, *40*, 3065–3072. [[PubMed](#)]
- Yu, C., Klein, S. A., & Levi, D. M. (2001). Surround modulation of perceived contrast and the role of brightness induction. *Journal of Vision*, *1*(1), 18–31, <http://journalofvision.org/1/1/3/>, doi:10.1167/1.1.3. [[PubMed](#)] [[Article](#)]
- Yu, C., Klein, S. A., & Levi, D. M. (2003). Cross and iso-oriented surrounds modulate the contrast response function: The effect of surround contrast. *Journal of Vision*, *3*(8), 527–540, <http://journalofvision.org/3/8/1/>, doi:10.1167/3.8.1. [[PubMed](#)] [[Article](#)]
- Yu, C., Klein, S. A., & Levi, D. M. (2004). Perceptual learning in contrast discrimination and the (minimal) role of context. *Journal of Vision*, *4*(3), 169–182, <http://journalofvision.org/4/3/4/>, doi:10.1167/4.3.4. [[PubMed](#)] [[Article](#)]
- Zenger, B., Braun, J., & Koch, C. (2000). Attentional effects on contrast detection in the presence of surround masks. *Vision Research*, *40*, 3717–3724. [[PubMed](#)]
- Zenger-Landolt, B., & Heeger, D. J. (2003). Response suppression in V1 agrees with psychophysics of surround masking. *Journal of Neuroscience*, *23*, 6884–6893. [[PubMed](#)] [[Article](#)]